Catal Lett (2012) 142:243–250
DOI 10.1007/s10562-011-0749-1

Towards the Development of Fiber-Based Oxidovanadium(IV) Catalysts for the Oxidation of Thioanisole

Ryan S. Walmsley · Samuel Chigome · Nelson Torto · Zenixole R. Tshentu

Received: 15 July 2011 / Accepted: 20 November 2011 / Published online: 6 December 2011

Abstract The catalytic activity of a series of *bis*-coordinated oxidovanadium(IV) complexes with 2-(4,5-diphenyl-1*H*-imidazol-2-yl)-4*R*-phenol ligands (R = NO_2, Br, H, MeO) was investigated for the oxidation of thioanisole by hydrogen peroxide in acetonitrile at 25°C. The substituent groups had a significant effect on the catalytic activity and followed the order $NO_2 > Br > H > MeO$, with the nitro (NO_2) derivative achieving >99% conversion after 10 min while the methoxy (MeO) derivative yielded the same result in 60 min. The nitro- and methoxy-substituted homogeneous catalysts were incorporated into polystyrene and electrospun to form nonwoven mats with fiber diameters in the range 0.33–1.98 μm. These vanadium incorporated fibers were subjected to a continuous flow system at a flow rate of 1 mL/h for the oxidation of thioanisole and the nitro-substituted catalyst showed excellent catalytic activity with conversions dropping from 99 to 93% in the 10th fraction while the drop was down to 88% for the methoxy-substituted catalyst.

Keywords Oxidovanadium · Oxidation · Sulfides · Electrospun nanofibers · Continuous flow

1 Introduction

The oxidation of sulfides has become a popular and useful reaction [1–4]. Not only does this reaction yield products which serve as intermediates in the synthesis of biologically active compounds [5], but it also holds importance for the petrochemical industry in the production of low sulfur fuels through oxidative desulfurization [6]. Several oxidants have been used for the oxidation of sulfides including but not limited to, molecular oxygen, peroxides and monoperoxysulfate [7]. Current economical and environmental concerns make hydrogen peroxide an attractive option due to its low cost and lack of harmful by-products, respectively [8]. Combining hydrogen peroxide with a transition metal catalyst provides further benefits including a reduced reaction time [9, 10], as well as the ability to manipulate product selectivity and chirality [11]. The use of vanadium catalysts for the oxidation of sulfides has attracted much interest in this regard. Both oxidovanadium(IV) [12] and dioxidovanadium(V) [13] complexes have been shown to facilitate the oxidation of not only sulfides but several organic substrates including alkanes and alkenes [14].

A great deal of research at the moment is focussed around immobilizing these homogeneous catalysts onto solid supports [15, 16]. Although homogeneous catalysts often exhibit improved activity over their heterogeneous counterparts, they are rarely applied to the chemical and petrochemical industries [6]. This is possibly due to the difficulty and expense of recovering homogeneous catalysts from the reaction solution. There are several materials that have proven to be useful supports for immobilizing vanadium catalysts, one of which is micro-spherical polystyrene-based resins [10–12]. These resins can be easily functionalized to provide sites for subsequent ligand and metal attachment. The catalytic surface area of these resins

---

Electronic supplementary material The online version of this article (doi:10.1007/s10562-011-0749-1) contains supplementary material, which is available to authorized users.

R. S. Walmsley · S. Chigome · N. Torto · Z. R. Tshentu (✉)
Department of Chemistry, Rhodes University, Grahamstown 6139, South Africa
e-mail: z.tshentu@ru.ac.za

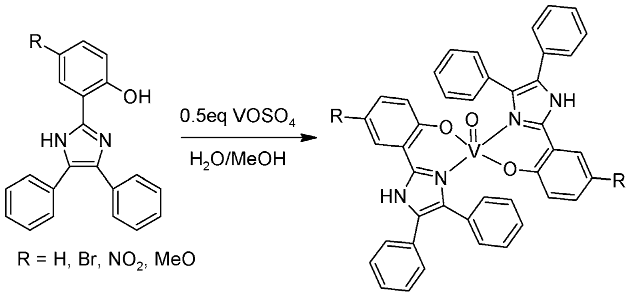

Scheme 1 Synthesis scheme of oxidovanadium(IV) complexes

can be increased by decreasing their diameter, however as one enters the nanometer domain, separation of the resins can become more difficult and centrifugation is often required [17]. Electrospun nanofibers have diameters in the nanometer region and intertwine to form a web-like structure or mat, making them very easy to separate from solution [18] as well as having possible application as membranes in membrane catalysis [19]. Most research in application of fibers in catalysis involves the deposition of metal nanoparticles on the surface of the fibers [20], or preparation of inorganic/metal oxide based fibers [21]. There are, however, no studies focusing on immobilization of coordination complexes onto nanofibers.

In this paper, a series of 2-(4,5-diphenyl-1*H*-imidazol-2-yl)-4*R*-phenol ligands and their corresponding *bis*-coordinated oxidovanadium(IV) complexes were prepared (Scheme 1) and characterized. The effect of the electron donating/withdrawing substituents on catalytic activity was evaluated. The homogeneous catalysts were then incorporated into polystyrene and electrospun to produce nanofiber mats. The catalytic performance of the incorporated catalysts was evaluated for the oxidation of thioanisole with hydrogen peroxide under continuous flow conditions.

2 Experimental

2.1 Materials and Instrumentation

Polystyrene (M_W, 192 000) and all other chemicals used were >98% purity and were purchased from either Sigma-Aldrich or Merck chemical company and used without further purification. Solvents were reagent grade.

The infrared spectra were recorded on either a Perkin Elmer 100 ATR-FTIR (4000–650 cm^{-1}) or Perkin Elmer 400 FT-IR spectrometer (4000–400 cm^{-1}). ^{1}H and ^{13}C NMR spectra of the ligands were recorded on a Bruker AMX 400 NMR MHz spectrometer and reported relative to tetramethylsilane (δ 0.00). Electronic spectra were recorded on a Perkin Elmer Lambda 25 UV–Vis spectrophotometer using 1 cm quartz cells and N,N-dimethylformamide (DMF) as the solvent. Microanalysis was carried out using a Vario Elementar Microcube ELIII. Catalyzed reactions were monitored using the Agilent 7890A gas chromatograph (GC), fitted with a flame ionization detector (FID) and a Zebron, ZB-5MSi, capillary column (30 m × 0.25 mm × 0.25 μm). Mass spectra were obtained using a Thermo-Finnigan GC–MS fitted with electron impact ionization. The morphology of the polymer fibers was investigated using a TESCAN Vega TS 5136 LM scanning electron microscope (SEM). The vanadium content was determined using a Thermo Electron (iCAP 6000 Series) inductively coupled plasma (ICP) spectrometer equipped with an OES detector. The wavelengths 290.88 nm, 292.40 nm, 309.31 nm, and 311.07 nm were chosen and triplicate analyses were performed at each wavelength. Aqueous hydrogen peroxide (H_2O_2) was standardized using a potassium permanganate titration [22] and found to have a concentration of 29.4% (wt%).

2.2 Preparation of Ligands

All substituted 2-(4,5-diphenyl-1*H*-imidazole-2-yl)phenol derivatives were prepared according to a literature procedure [14].

2.2.1 *2-(4,5-Diphenyl-1H-imidazol-2-yl)phenol (dpimH)*

Yield: 70%. Mp 203–204°C. Selected IR peaks (cm^{-1}): 3,189 m, 3,053 m, 1,601 m, 1,590 m, 1,552 m, 1,485 s, 1,216 s, 1,023 s, 766 vs, 691 vs. ^{1}H NMR (400 MHz, DMSO); δ 8.09 (br, d, 2H); 7.65 (m, 4H); 7.56 (m, 3H); 7.43 (m, 6H). ^{13}C NMR (100 MHz, DMSO): 159.4, 145.2, 136.0, 131.9, 130.8, 128.7, 128.4, 128.1, 127.6, 126.5, 126.4, 126.1. Anal. Calcd for $C_{21}H_{16}N_2O$: C, 80.75; H, 5.16; N, 8.97. Found: C, 80.17; H, 5.22; N, 8.87.

2.2.2 *4-Methoxy-2-(4,5-diphenyl-1H-imidazol-2-yl)phenol (dpimMeO)*

Yield: 86%. Mp 159–160°C. Selected IR peaks (cm^{-1}): 3,194 m, 3,048 m, 1,605 m, 1,586 m, 1,499 s, 1,224 s, 1,036 s, 764 vs, 696 vs. ^{1}H NMR (400 MHz, DMSO); δ 13.02 (s, 1H); 12.47 (s, 1H); 7.67 (s, 1H); 7.40 (m, 10H); 6.89 (m, 2H); 3.77 (s, 3H). ^{13}C NMR (100 MHz, DMSO): 151.9, 150.8, 145.8, 134.2, 133.6, 128.8, 127.3, 127.1, 126.7, 117.5, 116.9, 112.5, 108.8, 55.6. Anal. Calcd for $C_{22}H_{18}N_2O_2$: C, 77.17; H, 5.30; N, 8.18. Found: C, 77.10; H, 5.38; N, 8.09.

2.2.3 *4-Bromo-2-(4,5-diphenyl-1H-imidazol-2-yl)phenol (dpimBr)*

Yield: 71%. Mp 186–187°C. Selected IR peaks (cm^{-1}): 3,166 m, 3,043 m, 1,604 m, 1,579 m, 1,567 m, 1,484 s, 1,278 s, 1,254 m, 1,143 m, 1,074 s, 1,026 m, 762 vs, 696 vs. ^{1}H NMR (400 MHz, DMSO); δ 13.11 (br, s, 1H); 8.30 (s, 1H); 7.53–7.39 (m, 11H); 6.95 (d, 1H). ^{13}C NMR (100 MHz, DMSO): 167.3, 156.7, 154.9, 145.3, 133.2, 129.5, 128.7, 128.3, 127.9, 127.7, 119.9, 115.6. Anal. Calcd for $C_{21}H_{15}BrN_2O$: C, 64.46; H, 3.86; N, 7.16. Found: C, 64.26; H, 3.90; N, 7.25.

2.2.4 *4-Nitro-2-(4,5-diphenyl-1H-imidazol-2-yl)phenol (dpimNO$_2$)*

Yield: 62%. Mp 219–220°C. Selected IR peaks (cm^{-1}): 3,289 m, 3,055 m, 1,615w, 1,594 m, 1,584 m, 1,471 s, 1,336 s, 1,129 s, 1,074 m, 1,024 m, 763 s, 739 s, 687 s. ^{1}H NMR (400 MHz, DMSO); δ 13.9 (br, s, 1H); 9.15 (s, 1H); 8.17 (d, 1H); 7.54 (m, 4H); 7.43 (m, 4H); 7.38 (m, 2H); 7.16 (d, 1H). ^{13}C NMR (100 MHz, DMSO): 165.5, 157.3, 154.3, 144.4, 133.2, 130.1, 128.8, 127.9, 127.6, 127.3, 126.9, 120.3, 114.5. Anal. Calcd for $C_{21}H_{15}N_3O_3$: C, 70.58; H, 4.23; N, 11.76. Found: C, 70.29; H, 4.18; N, 11.46.

2.3 Preparation of Oxidovanadium(IV) Complexes

2.3.1 *[VO(dpimH)$_2$]*

The ligand dpimH (0.31 g, 1 mmol) was dissolved in warm methanol (10 mL). Vanadyl sulfate (0.1 g, 0.45 mmol) was dissolved in 3 mL of a methanol/water (2:1 ratio) solution. This solution was then added dropwise to the methanolic ligand solution. The mixture was stirred for 4 h at room temperature. The resultant blue-green precipitate was collected by filtration and washed with water and methanol and then dried at 100°C. Yield: 62%. Selected IR peaks (cm^{-1}): 1,604 m, 1,589 w, 1,565 m, 1,477 s, 1,456 m, 1,303 m, 1,251 s, 1,139 s, 1,025 m, 945 m, 869 s, 750 s, 694 s. UV–Vis (DMF) λ_{max} (ε, M^{-1}cm^{-1}): 527 (53), 632 (31), 836 (43). Anal. Calcd for $C_{42}H_{30}N_4O_3V.2H_2O$: C, 69.51; H, 4.72; N, 7.72. Found: C, 69.59; H, 4.71; N, 7.64.

2.3.2 *[VO(dpimMeO)$_2$]*

This compound was prepared as for 2.3.1 above except the ligand dpimMeO was used. The resultant compound was a yellow-green solid. Yield: 64%. Selected IR peaks (cm^{-1}): 1,587 m, 1,489 s, 1,225 s, 1,034 m, 975 m, 764 s, 692 s. UV–Vis (DMF) λ_{max} (ε, M^{-1}cm^{-1}): 515 (78), 625 (48), 844 (55). Anal. Calcd for $C_{44}H_{34}N_4O_5V.H_2O$: C, 68.84; H, 4.73; N, 7.30. Found: C, 68.71; H, 4.81; N, 7.26.

2.3.3 *[VO(dpimBr)$_2$]*

This compound was prepared as for 2.3.1 above except the ligand dpimBr was used. The resultant compound was a blue-green solid. Yield: 59%. Selected IR peaks (cm^{-1}): 1,601 m, 1,561 m, 1,475 s, 1,294 m, 1,250 m, 1,142 m, 1,028 m, 958 m, 696 s. UV–Vis (DMF) λ_{max} (ε, M^{-1}cm^{-1}): 522 (54), 639 (30), 823 (42). Anal. Calcd for $C_{42}H_{28}Br_2N_4O_3V.2H_2O$: C, 57.20; H, 3.59; N, 6.30. Found: C, 57.10; H, 3.65; N, 6.34.

2.3.4 *[VO(dpimNO$_2$)$_2$]*

This compound was prepared as for 2.3.1 above except the ligand dpimNO$_2$ was used. The resultant compound was an orange-green solid. Yield: 45%. Selected IR peaks (cm^{-1}): 1,608 m, 1,579 m, 1,486 m, 1,331 m, 1,138 m, 1,072 m, 964 m, 692 s. UV–Vis (DMF) λ_{max} (ε, M^{-1}cm^{-1}): 613 (49), 849 (55). Anal. Calcd for $C_{42}H_{32}N_6O_9V.2H_2O$: C, 61.84; H, 3.95; N, 10.30. Found: C, 62.06; H, 4.13; N, 10.08.

2.4 Electrospinning

2.4.1 *PS-25*

A mass of 1.25 g of polystyrene (PS) was dissolved in 5 mL of a DMF:THF (4:1) solvent mixture to make a 25% PS solution, which was subsequently stirred for 24 h to ensure homogeneity. The solution was then transferred to a 20 mL syringe and electrospun. The voltage applied to the needle tip was 20 kV and the tip to collector distance was 15 cm. The internal diameter of the needle was 1 mm and the flow rate was 1 mL/h. The white fibers were collected by vertical electrospinning on a piece of aluminum foil that was grounded (Fig. 1). Selected IR peaks (cm^{-1}): 1,655 s,

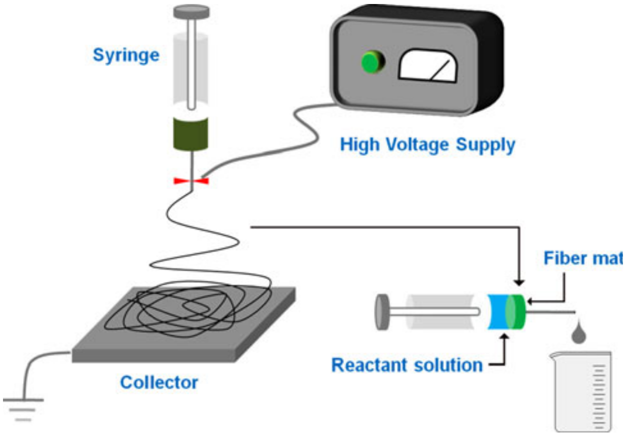

Fig. 1 An illustration of a typical electrospinning and continuous flow reaction set-up. The polymer solution was placed in a syringe connected to a high voltage supply. A high voltage was applied at the needle tip and the resultant fibers were collected on a grounded collector. These fibers were then packed in a syringe, and a sulfide-containing reactant solution passed through the fibers at a controlled rate in a continuous flow fashion

1,492 s, 1,451 s, 749 vs, 696 vs. Anal. Found: C, 84.68; H, 8.08.

2.4.2 *PS-25-[VO(dpimMeO)$_2$]*

Same as above (2.4.1) except [VO(dpimMeO)$_2$] (0.25 g, 20 wt% relative to PS) was added to the mixture. The resulting fiber mat was a light green color. Selected IR peaks (cm^{-1}): 1,491 s, 1,451 s, 1,281 w, 975 vw, 811 w, 694 vs. Anal. Found: C, 73.36; H, 7.43; N, 3.32; V, 3.00.

2.4.3 *PS-15-[VO(dpimMeO)$_2$]*

Same as above (2.4.2) except a mass of 1.25 g of PS was dissolved in 8.3 mL of a DMF: tetrahydrofuran (THF) (4:1) solution to make a 15% PS solution. The internal needle diameter was 0.5 mm and the flow rate was kept constant at 0.5 mL/h. The resulting fiber mat was a green color. Anal. Found: C, 85.85; H, 7.31; N, 1.28; V, 1.19.

2.4.4 *PS-25-[VO(dpimNO$_2$)$_2$]*

Same as for (2.4.2) except [VO(dpimNO$_2$)$_2$] (0.25 g, 20 wt%) was used. The flow rate was reduced to 0.6 mL/h. The resulting fiber mat was a yellow color. Selected IR peaks (cm^{-1}): 1,579 m, 1,182 vw, 1,138 w, 1,070 w, 1,025 w, 987 vw, 966 vw, 891 vw, 840 vw. Anal. Found: C, 87.22; H, 7.61; N, 1.41; V, 0.86.

2.4.5 *PS-15-[VO(dpimNO$_2$)$_2$]*

Same as for (2.4.3), except that [VO(dpimNO$_2$)$_2$] was included in the mixture. The resulting fiber mat was yellow in color. Anal. Found: C, 85.93; H, 7.45; N, 1.41; V, 0.84.

2.5 Catalytic Activity Studies

2.5.1 *Batch Experiments*

In a typical homogeneous catalytic oxidation experiment, 20 mL of acetonitrile and the oxidovanadium complex (0.25 mol%) were mixed in a 50 mL round bottom flask. The temperature of the reaction was fixed at 25($\pm$1)°C by use of an external temperature probe. The oxidant, H_2O_2 (2 mol eq), was added followed by thioanisole (10 mmol) while the reaction was stirred at a constant rate of 300 rpm. Aliquots were withdrawn at 10 min time intervals and analyzed by GC.

2.5.2 *Continuous Flow Experiments*

The catalytic activity of the polymer-incorporated oxidovanadium(IV) complexes was also evaluated using a continuous flow approach. The fibers (0.010 g) were packed between two filter disks (Whatmann no. 1) in a 10 mL syringe. In a separate flask; H_2O_2 (2 mol eq), thioanisole (0.5 mmol) and solvent mixture were mixed for 5 min. This reactant solution was poured into the syringe. The solution was passed through the fibers at a controlled rate using a syringe pump (New Era, NE-1000). Fractions of 1 mL were collected and analyzed using GC.

3 Results and Discussion

3.1 Synthesis and Characterization of Catalysts

The ligands chosen in this study were based on the 2-(2′-hydroxyphenyl)-1*H*-imidazoline ligand used in our previous work [10] with two major exceptions. Two extra phenyl groups were added to provide additional stability through π-π interactions with polystyrene [23] and the substituent at the *para*-position of the phenol ring was varied to assess the effect of electron withdrawing/donating groups on the catalytic activity. All the complexes displayed characteristic $\nu(V=O)$ stretches occurring between 945 and 975 cm^{-1}, which is within the reported range for oxidovanadium(IV) compounds [24]. The UV–Vis spectra of all of the complexes besides [VO(dpimNO$_2$)$_2$] displayed three d–d transitions, commonly observed for a square pyramidal oxovanadium(IV) complexes [25]. The first transition appeared between 515 and 527 nm $\left(d_{xy} \rightarrow d_{z^2}\right)$, the second between 613 and 639 nm $\left(d_{xy} \rightarrow d_{x^2-y^2}\right)$ and the third between 823 and 849 nm $\left(d_{xy} \rightarrow d_{xz}, d_{yz}\right)$. Although the lowering of symmetry from C_{4v} to C_{2v} lifts the degeneracy of the d_{xz} and d_{yz} orbitals this is often not observed experimentally. The first d–d transition for [VO(dpimNO$_2$)$_2$] was hidden beneath the intense charge transfer band appearing in this region (Fig. 2).

The homogeneous catalysts were incorporated into polystyrene by mixing them together in a solvent mixture of DMF/THF. This simple method offers practical advantages in that no chemical modification of the homogeneous catalysts is required [26]. Fibers of the composite material were then produced by using the electrospinning technique [27]. The change in color of the fibers (Fig. 3), along with elemental (Sect. 2.4) and infrared data (Fig. S1) confirms the presence of the catalysts within the polymer fibers.

The amount of catalyst added to the polystyrene solution was kept constant at 20% (wt% with respect to polystyrene) while the percentage of polystyrene was adjusted to tune the fiber diameters. Inclusion of the oxidovanadium complexes in the polymer solution allowed for the production of smooth fibers at both 25% (w/v) and the lower

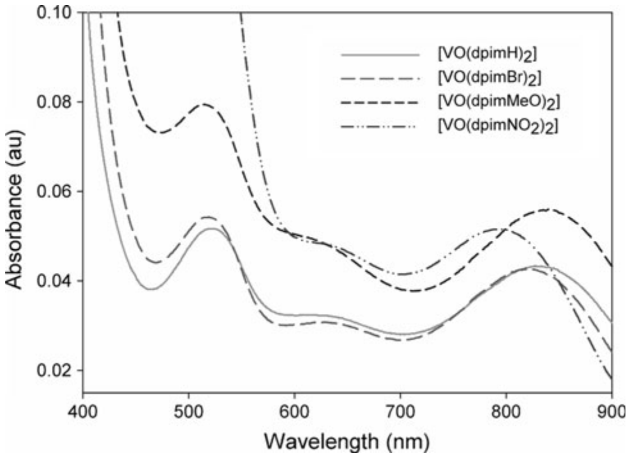

Fig. 2 UV/Vis spectra of the oxidovanadium(IV) complexes

15% polystyrene concentrations (Fig. 4) while for the pure polystyrene smooth fibers were only obtained at the higher 25% concentration, a trend commonly observed [28]. The fiber diameters were measured from an average of 20 fibers; the 25% polystyrene-based fibers, PS-25-[VO(dpimMeO)$_2$] and PS-25-[VO(dpimNO$_2$)$_2$], had average fiber diameters of 1.37 and 1.98 µm, respectively, while for the 15% polystyrene-based fibers, PS-15-[VO(dpimMeO)$_2$] and PS-15-[VO(dpimNO$_2$)$_2$], it was 0.33 and 0.51 µm, respectively.

3.2 Catalytic Activity of Homogeneous Catalysts

In this study, the activity of the oxidovanadium(IV) catalysts was evaluated for the H_2O_2 facilitated oxidation of thioanisole. The oxidation products detected were methyl phenyl sulfoxide and methyl phenyl sulfone as confirmed by comparison of retention times with standards and by GC/MS. The general reaction and proposed catalytic mechanism is shown in Scheme 2. From this scheme it is evident that although the prepared oxidovanadium(IV) complexes are referred to as catalysts, they are really catalyst precursors which are converted to the active species in peroxide conditions.

The amount of catalyst and H_2O_2 was kept constant at 0.25 mol% and two equivalents relative to thioanisole, respectively, while the temperature was kept at 25 (± 1)°C, since we have found these conditions to be effective in the past [10, 12]. It was observed that the electron withdrawing/donating substituents on the *para*-position of the phenol group of the ligand had a significant impact on the overall catalytic activity and selectivity. The nitro substituted homogeneous catalyst showed the best activity with a >99% conversion of thioanisole, being attained after just 10 min at 25°C, compared to the electron donating MeO-substituted catalyst, which achieved the same result in 60 min (Fig. 5). The activity of the catalysts showed the following trend as shown by their turn-over frequencies (TOF); NO_2 (2,400 h^{-1}) > Br (800 h^{-1}) > H (600 h^{-1}) > MeO (480 h^{-1}). When the solvent mixture was changed from pure CH_3CN to a mixture of CH_3CN/H_2O the conversion dropped slightly, while the selectivity shifted slightly to favor the formation of sulfone (Table S1). In the absence of catalyst low conversions were obtained.

The introduction of electron withdrawing groups *para* on the phenol group of the ligand seems to improve the activity perhaps by rendering the metal center electron deficient. The product selectivity was also dependant on the substituent groups. The milder MeO-substituted catalyst displayed higher selectivity towards the formation of methyl phenyl sulfoxide whereas the NO_2-substituted derivative seemed to favor the formation of the sulfone, especially as time progressed (Fig. 6). This was expected since the more active NO_2-substituted derivative further oxidizes the sulfoxide to the sulfone. A table containing product selectivity and overall conversions for the catalyzed reactions can be found in the electronic supplementary information.

Fig. 3 Picture of the electrospun fibers, from left to right; PS-25, PS-15-[VO(dpimMeO)$_2$] and PS-15-[VO(dpimNO$_2$)$_2$]

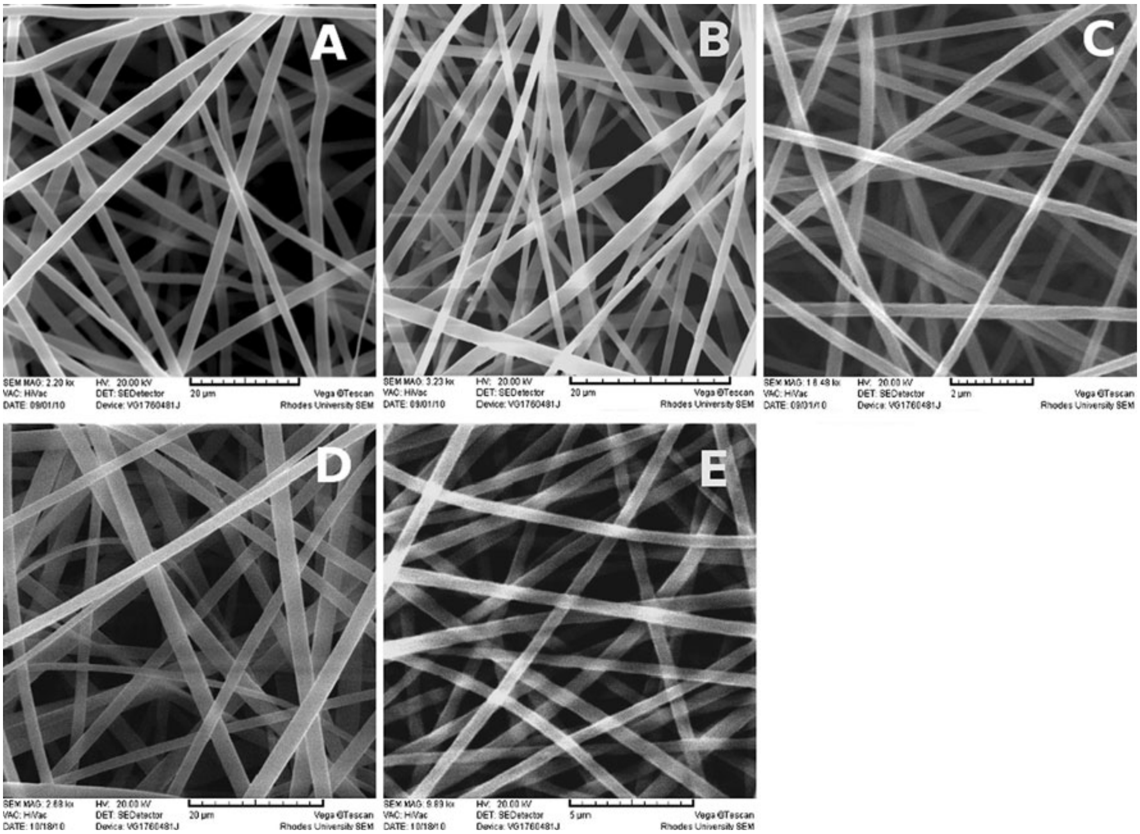

Fig. 4 SEM images of **a** PS-25. **b** PS-25-[VO(dpimMeO)$_2$]. **c** PS-15-[VO(dpimMeO) $_2$]. **d** PS-25-[VO(dpimNO$_2$)$_2$]. **e** PS-15-[VO(dpimNO$_2$)$_2$]

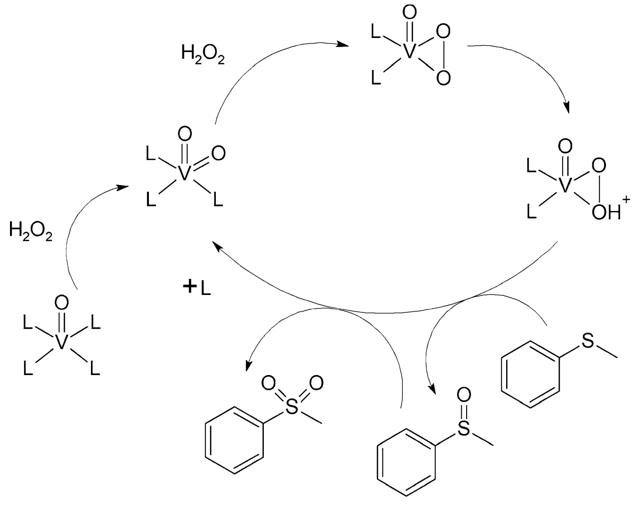

Scheme 2 Outline of the catalytic reaction [16] and general reaction for the oxidation of thioanisole to methyl phenyl sulfoxide and methyl phenyl sulfone

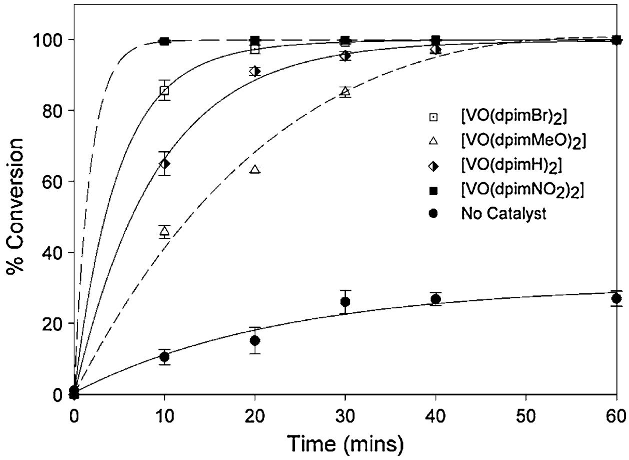

Fig. 5 Ligand substituent effect on catalytic activity. Conditions: Catalyst (0.25 mol%), thioanisole (10 mmol), H_2O_2 (2 eq, 20 mmol), CH_3CN (20 mL), and at 25°C

3.3 Catalytic Activity of Nanofiber-Incorporated Catalysts

Rather than applying these fibers in a batch reaction as was the case for the homogeneous catalysts, a continuous flow approach was chosen since the highly porous nature of the fiber-mats was well suited to this approach. Furthermore, the non-crosslinked polystyrene fibers are susceptible to breaking by mechanical agitation with the magnetic stirrer bar. Since the oxidovanadium complexes were highly insoluble in water, the solvent used in the catalyzed

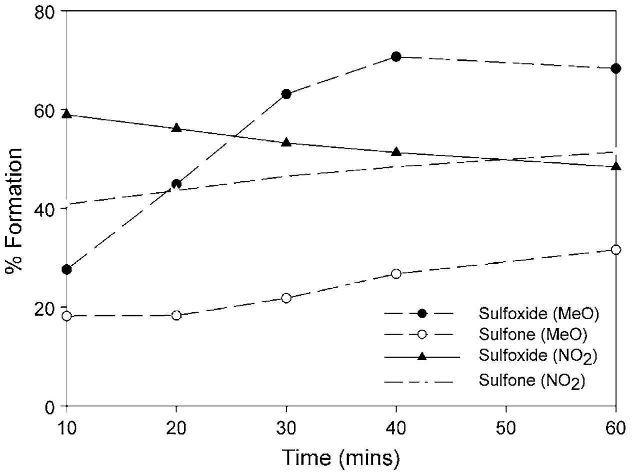

Fig. 6 Product selectivity for the oxidation of thioanisole. Conditions: Catalyst (0.25 mol%), thioanisole (10 mmol), H_2O_2 (2 eq, 20 mmol), CH_3CN (20 mL), and at 25°C

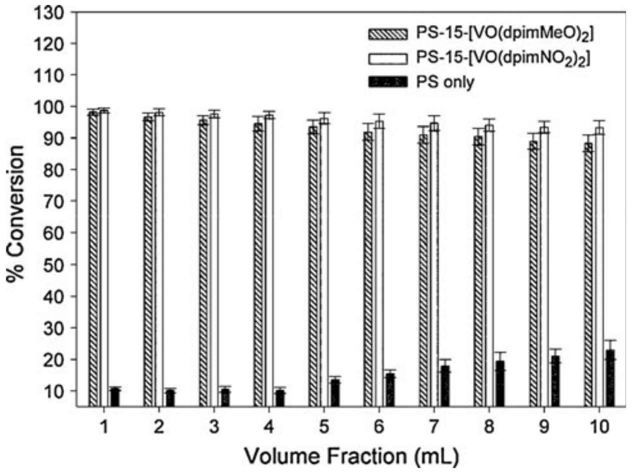

Fig. 7 Oxidation of thioanisole under continuous flow conditions. Conditions: thioanisole (50 mM), H_2O_2 (100 mM), PS-15-[VO(dpimNO$_2$)$_2$] (0.01 g) and PS-15-[VO(dpimMeO)$_2$] (0.01 g) of catalyst in 1:1 CH_3CN/H_2O; 25°C; flow rate = 1 mL/h

reactions was changed to a mixture of CH_3CN/water (1:1), rather than pure CH_3CN to limit leaching from the polymer.

The effect of the flow rate, fiber diameter and catalyst type on the reaction was investigated. Only [VO(dpimMeO)$_2$] and [VO(dpimNO$_2$)$_2$], which were least and the most active catalysts, respectively, were studied by this method to assess if any impact on catalytic activity would be observed. An increase in flow rate from 0.5 to 1 mL/h resulted in an improvement in % conversions but a further increase to 1.5 mL/h resulted in a moderate drop in conversion and so subsequent reactions were performed at 1 mL/h (see the supplementary information). The different diameters of the fibers (0.33 and 1.37 µm for PS-15-[VO(dpimMeO)$_2$] and PS-25-[VO(dpimMeO)$_2$], respectively, and 0.51 and 1.98 µm for PS-15-[VO(dpimNO$_2$)$_2$] and PS-25-[VO(dpimNO$_2$)$_2$], respectively) had no observable effect on catalytic activity. As shown in Fig. 7, PS-15-[VO(dpimNO$_2$)$_2$] showed good catalytic activity, with the conversion of thioanisole remaining above 93% over the 10 h (or 10 mL) period studied. As has been the trend with homogeneous catalysts (Fig. 5), PS-15-[VO(dpimMeO)$_2$] was also slightly less active than PS-15-[VO(dpimNO$_2$)$_2$] with conversions dropping to 87.7% in the 10th fraction. The greater activity of the NO$_2$-substituted catalysts resulted in slightly higher formation of the sulfone compared to the MeO-substituted catalyst, for the same reason as discussed for the homogeneous catalysts. When using un-functionalized polystyrene fibers (PS-25) a maximum conversion of 22.9% was obtained on the last fraction intimating that the presence of the catalyst is crucial for expediting these oxidation reactions. More data regarding the effect of the above mentioned conditions on selectivity and overall conversion may be found in Table S1 and Fig. S2.

For both catalysts, the activity drops slightly after time and for this reason the leaching of vanadium from the polymer was quantified. Each of the 1 mL product fractions collected from the continuous flow system were evaporated to dryness. The remaining residue was digested in 0.5 mL of nitric acid (Ultrapure, 69%) for 24 h and diluted with deionised water to a total volume of 15 mL. This solution was passed through a Millipore filter (0.45 µM) and analyzed by ICP-OES. An average of 3.8 (± 1.4)% of vanadium was lost in each fraction which corresponds with the observed drop in activity. This study has led us to begin work on covalently linking the ligands to the polymers and electrospinning their solutions prior to the introduction of oxidovanadium(IV). It is hoped that this will improve the stability of the catalysts and address the vanadium leaching observed in this incorporation method.

4 Conclusions

A series of novel, catalytically active, oxidovanadium(IV) complexes with electron withdrawing/donating substituents *para* to the phenol group of the ligand, were successfully prepared and evaluated for the catalytic oxidation of thioanisole. All complexes successfully catalyzed this reaction; however, inclusion of an electron withdrawing group on the ligand significantly improved the activity. The homogeneous catalysts were incorporated into polystyrene and electrospun into nanofibers. The catalytic activity of these fibers was evaluated using a continuous flow set up and under these conditions near quantitative conversion of thioanisole was observed for an extended period of time. Despite a small drop in catalytic activity of these fibers over time, their excellent activity makes them an attractive option that needs further improvements with respect to stability before consideration for real application in desulfurization processes.

Acknowledgments We thank Sasol and the South African National Research Foundation for funding. We also thank the SEM-unit (Rhodes University) for use of the Electron Microscope, and the DST/Mintek National Innovation Centre (Rhodes University) for the microanalysis data. R. Walmsley would like to acknowledge his colleagues in the laboratory for their input.

References

1. Choudary BM, Bharathi B, Venkat Reddy C, Lakshimi Kantam M (2002) J Chem Soc, Perkin Trans 1:2069
2. Kumar Karmee S, Greiner L, Kraynov A, Müller TE, Niemeijer B, Leitner W (2010) Chem Commun 46:6705
3. Ji H-B, Wang TT, Wang L-F, Fang Y-X (2007) React Kinet Catal Lett 90:259
4. Panda MK, Shaikh MM, Ghosh P (2010) Dalton Trans 39:2428
5. Kaczorowska K, Kolarska Z, Mitka K, Kowalski P (2005) Tetrahedron 61:8315
6. Maurya MR, Arya A, Kumar A, Kuznetsov ML, Avecilla F, Costa PJ (2010) Inorg Chem 49:6586
7. Velusamy S, Srinivasan A, Punniyamurthy T (2006) Tetrahedron Lett 47:923
8. Bagchi D, Stohs SJ, Downs BW, Bagchi M, Preuss HG (2003) Toxicology 186:175
9. Sherrington DC (1987) Pure Appl Chem 60:401
10. Tshentu ZR, Togo C, Walmsley RS (2010) J Mol Catal A: Chem 318:30
11. Canali L, Sherrington DC, Deleuze H (1999) React Funct Polym 40:155
12. Walmsley RS, Tshentu ZR (2010) S Afr J Chem 63:95
13. Maurya MR, Kumar A, Ebel M, Rehder D (2006) Inorg Chem 45:5924
14. Eseola AO, Li W, Gao R, Zhang M, Hao T, Liang, Obl-Egbedi NO, Sun WH (2009) Inorg Chem 48:9133
15. Maurya MR, Arya A, Kumar A, Pessoa JC (2009) Dalton Trans 28:2185
16. da Silva JAL, da Silva JJRF, Pombeiro AJL (2011) Coord Chem Rev 255:2232
17. Wang Y, Biradar AV, Duncan CT, Asefa T (2010) J Mater Chem 20:7834
18. Huang ZM, Zhang YZ, Kotaki M, Ramakrishna S (2003) Compos Sci Technol 63:2223
19. Formo E, Yavuz MS, Lee EP, Lane L, Xia Y (2009) J Mater Chem 19:3878
20. Patel AC, Li S, Wang C, Zhang W, Wei Y (2007) Chem Mater 19:1231
21. Xu S, Sun D, Liu H, Wang X, Yan X (2011) Catal Commun 12:514
22. Reichert JS, McNeight SA, Rudel HW (1939) Ind Eng Chem 11:194
23. Huang J, Huang K, Liu S, Luo Q, Shi S (2008) J Colloid Interf Sci 317:434
24. Wilkinson G, Gillard RD, McCleverty JA (1987) Comprehensive Coordination Chemistry. Pergamon Press, New York
25. Selbin J (1965) Chem Rev 65:153
26. Caselli A, Buonomenna G, de Baldironi F, Laera L, Fantauzzi S, Ragaini F, Gallo E, Golemme G, Cenini S, Drioli E (2010) J Mol Catal A: Chem 317:72
27. Greiner A, Wendorff JH (2007) Angew Chem Int Ed 46:5670
28. Eda G, Shivkumar S (2007) J Appl Polym Sci 106:475